Pharmacophore modeling of diverse classes of p38 MAP kinase inhibitors

ARTICLE *in* EUROPEAN JOURNAL OF MEDICINAL CHEMISTRY · MARCH 2008

Impact Factor: 3.45 · DOI: 10.1016/j.ejmech.2008.02.014 · Source: PubMed

Available online at www.sciencedirect.com
ScienceDirect
European Journal of Medicinal Chemistry 43 (2008) 2870–2876
EUROPEAN JOURNAL OF MEDICINAL CHEMISTRY
http://www.elsevier.com/locate/ejmech

Original article

Pharmacophore modeling of diverse classes of p38 MAP kinase inhibitors

Rituparna Sarma [a,*], Sharat Sinha [a], Muttineni Ravikumar [a], Madala Kishore Kumar [a], S.K. Mahmood [b]

[a] *Biocampus, GVK Biosciences Pvt. Ltd. S-1, Phase-1, Technocrats Industrial Estate, Balanagar, Hyderabad 500 037, A.P., India*
[b] *Bioinformatics Division, Environmental Microbiology Lab, Department of Botany, Osmania University, Hyderabad 500 007, A.P., India*

Received 11 October 2007; received in revised form 3 February 2008; accepted 7 February 2008
Available online 29 February 2008

Abstract

Mitogen-activated protein (MAP) p38 kinase is a serine–threonine protein kinase and its inhibitors are useful in the treatment of inflammatory diseases. Pharmacophore models were developed using HypoGen program of Catalyst with diverse classes of p38 MAP kinase inhibitors. The best pharmacophore hypothesis (Hypo1) with hydrogen-bond acceptor (HBA), hydrophobic (HY), hydrogen-bond donor (HBD), and ring aromatic (RA) as features has correlation coefficient of 0.959, root mean square deviation (RMSD) of 1.069 and configuration cost of 14.536. The model was validated using test set containing 119 compounds and had high correlation coefficient of 0.851. The results demonstrate that results obtained in this study can be considered to be useful and reliable tools in identifying structurally diverse compounds with desired biological activity.

Keywords: p38 MAP kinase; Catalyst; Pharmacophore

1. Introduction

The mitogen-activated protein (MAP) p38 kinase is a highly conserved proline-directed serine–threonine protein kinase which is implicated in most of the processes critical to inflammatory responses. p38 MAP kinase plays a very important role in diseases, viz., asthma, osteoarthritis and rheumatoid arthritis, a chronic obstructive pulmonary disease, primarily located in the synovial joints, leading to destruction of the cartilage and bone. p38 MAP kinase belongs to the superfamily of MAP kinases.

In response to a variety of stress stimuli (heat, UV light, lipopolysaccharide, high osmolarity), p38 MAP kinase is activated via dual phosphorylation of the TGY motif in the activation loop of the enzyme. Upon activation, p38 MAP kinase phosphorylates a number of downstream substrates, thereby regulating the synthesis of several important pro-inflammatory cytokines such as tumor necrosis factor-α (TNF-α) and interleukin-1 (IL-1). TNF-α inhibition has represented a fundamental role in the control of chronic inflammatory diseases such as rheumatoid arthritis. Therefore, the inhibition of p38 MAP kinase would potentially prevent the underlying pathophysiology in the inflammatory diseases, which makes p38 MAP kinase an attractive target for drug discovery [1,2].

In the present study, we have generated pharmacophore model using Catalyst [3,4] software for a diverse set of molecules as p38 MAP kinase inhibitors with an aim to obtain pharmacophore model that would provide a hypothetical picture of the chemical features responsible for activity. This in turn would be able to provide useful knowledge for developing potentially new and active drug candidates targeting the p38 MAP kinase, which can be useful as anti-inflammatory agents. Through this work, we plan to develop a valid pharmacophore model with chemically diverse set of compounds which is useful for designing of highly active inhibitors and also in virtual screening of new compounds targeting p38 MAP kinase.

* Corresponding author. Tel: +91 9908814521; fax: +91 40 23721010.
E-mail address: rituparna.sarma@gmail.com (R. Sarma).

0223-5234/$ - see front matter © 2008 Elsevier Masson SAS. All rights reserved.
doi:10.1016/j.ejmech.2008.02.014

Table 1
Pharmacophore models generated by HypoGen algorithm are listed

Hypothesis no.[a]	Total cost	Cost difference (null cost – total cost)	Error cost	RMS	Correlation (r)	Features[b]
1	141.995	163.797	118.061	1.069	0.959	HBA, HY, RA, RA
2	151.600	154.192	126.874	1.315	0.937	HBA, HY, RA, RA
3	157.270	148.522	134.576	1.498	0.916	HBA, HY, RA, RA
4	163.306	142.486	141.568	1.646	0.897	HBA, HY, RA, RA
5	168.052	137.740	145.581	1.726	0.886	HBA, HY, RA, RA
6	168.901	136.891	153.037	1.864	0.863	HBA, HY, HY, HY, RA
7	168.956	136.836	141.779	1.650	0.898	HBA, HY, RA, RA
8	170.350	135.442	150.824	1.824	0.870	HBA, HY, RA, RA
9	170.619	135.173	154.824	1.896	0.858	HBA, HY, HY, HY, RA
10	172.412	133.380	152.767	1.859	0.865	HBA, HY, RA, RA

[a] Null cost − 305.792, fixed cost − 116.569, configuration − 14.536, and weight − 1.125.
[b] HBA, hydrogen-bond acceptor; HY, hydrophobic feature; HBD, hydrogen-bond donor; and RA, ring aromatic.

2. Materials and methods

2.1. Selection of molecules

We selected a set of 149 compounds which are reported to be inhibitors of p38 MAP kinase. The inhibitory activity of these compounds [5–24], expressed as IC_{50} (i.e., concentration of compound required to inhibit 50% of p38 MAP kinase activity) was taken for the whole process. The activity reported for the compounds was measured according to same assay procedures. The IC_{50} values spanned across a wide range from 0.2 to 13 00 000 nM. Of these 149 compounds, 30 compounds were taken as training set (Table 2) and the rest of the 119 compounds as test set (Table 1S).

2.2. Molecular modeling

The geometry of a compound is built with the Catalyst builder and optimized by the CHARMM [25] like force field. All of the molecules were built using the builder module of Cerius2 [24]. All of the structures were minimized using the steepest descent algorithm with a convergence gradient value of 0.001 kcal/mol. Partial atomic charges were calculated using the Gasteiger method [26]. Further geometry optimization was carried out for each compound with the MOPAC 6 package using the semi-empirical AM1 Hamiltonian [27].

2.3. Pharmacophore modeling

Multiple acceptable conformations were generated for all ligands within the Catalyst ConFirm module using the "Poling" algorithm. A maximum of 250 conformations were generated for each molecule within an energy threshold of 20.0 kcal/mol above the global energy minimum. Instead of using just the lowest energy conformation of each compound, all conformational models for each molecule in training set were used in Catalyst for pharmacophore hypothesis generation. The training set molecules (30) associated with their conformations was submitted to the Catalyst hypothesis generation (HypoGen) (Chart 1, Table 1). Features such as hydrogen-bond acceptor (HBA), hydrophobic feature (HY), hydrogen-bond donor (HBD), ring aromatic (RA) features were included for the pharmacophore generation on the basis of common features present in the study molecules. The statistical parameters such as cost values determine the significance

Table 2
Experimental IC_{50} data and predicted IC_{50} data of 24 training set molecules based on top ranked hypothesis (Hypo1)

Compound no.	IC_{50} (nM)		Experimental activity scale[a]	Estimated activity scale[a]	Error factor[b]	Fit value[c]
	Experimental	Estimated				
2	49	56	++	++	+1.1	9.67
8	8	3.5	+++	+++	−2.3	10.87
12	170	100	+	++	−1.7	9.41
17	8	18	+++	++	+2.3	10.15
22	4700	840	+	+	−5.6	8.49
25	1300	430	+	+	−3.0	8.78
27	0.5	0.44	+++	+++	−1.1	11.77
30	0.6	0.34	+++	+++	−1.8	11.88
31	0.2	0.25	+++	+++	+1.3	12.01
34	22	310	++	+	+14.0	8.92
36	6	13	+++	++	+2.1	10.31
38	2	1	+++	+++	−2.0	11.41
40	990	990	+	+	+1.0	8.41
51	14	130	++	+	+9.2	9.30
61	140	360	+	+	+2.6	8.85
66	1 300 000	1 80 000	+	+	−7.3	6.16
67	1 000 000	2 60 000	+	+	−3.9	6.00
69	44 000	80 000	+	+	+1.8	6.51
70	200 000	90 000	+	+	−2.2	6.46
71	24 000	4400	+	+	−5.5	7.77
73	65	380	++	+	+5.9	8.83
74	350	910	+	+	+2.6	8.45
80	630	1000	+	+	+1.7	8.39
89	470	130	+	+	−3.7	9.30
106	1.4	2	+++	+++	+1.4	11.11
113	110	110	+	+	−1.0	9.38
116	270	270	+	+	+1.0	8.98
131	40	210	++	+	+5.2	9.09
143	200	380	+	+	+1.9	8.83
146	6600	1400	+	+	−4.6	8.25

[a] Activity scale: most active (<10 nM, +++); moderately active (10–100 nM, ++); and inactive (>100 nM, +).
[b] The error factor is computed as the ratio of the measured activity to the activity estimated by the hypothesis or the inverse if estimated is greater than measured.
[c] Fit value indicates how well the features in the pharmacophore overlap the chemical features in the molecule.

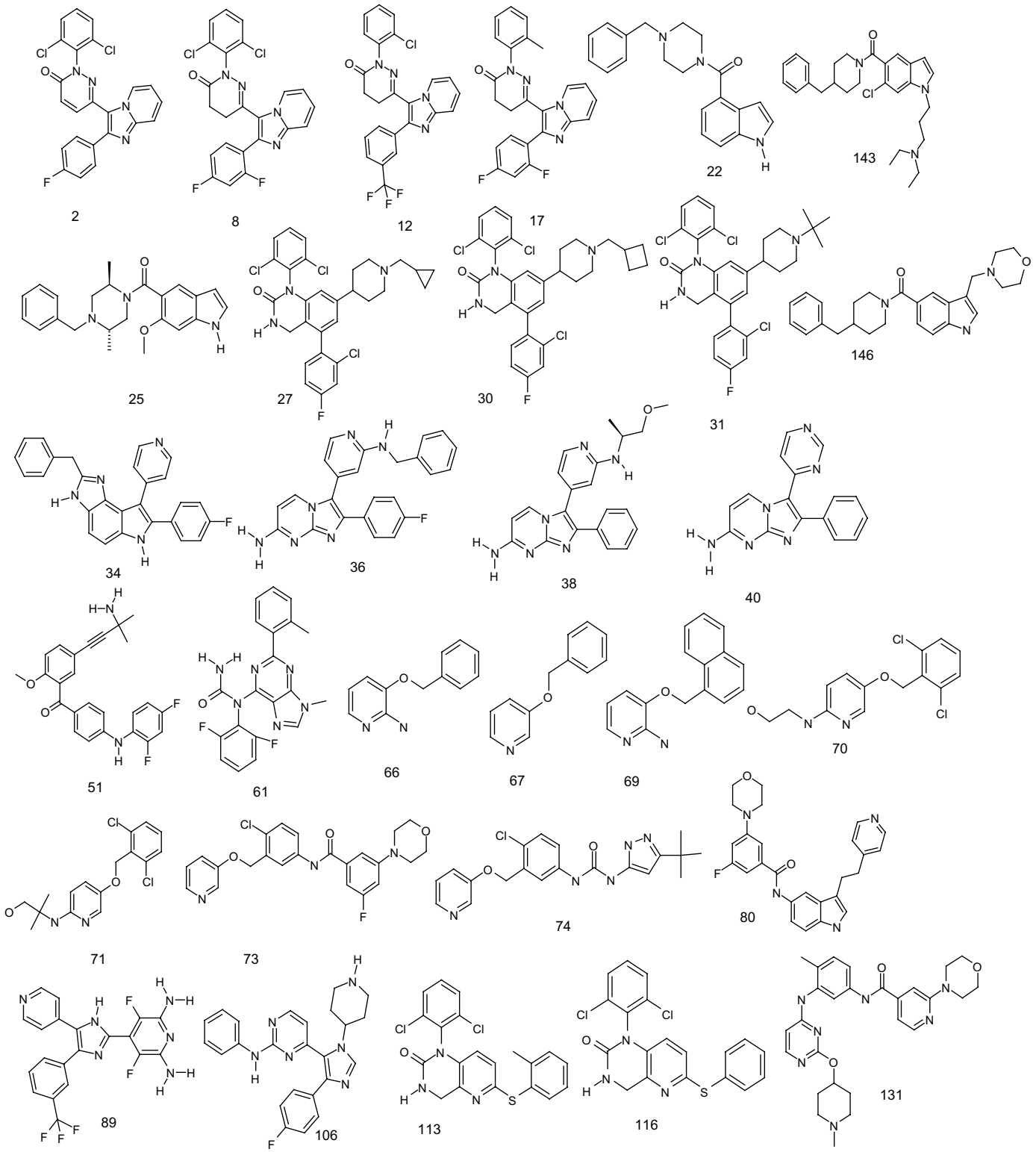

Chart 1. Training set molecules used in HypoGen studies.

of the model. Ten pharmacophore models with significant statistical parameters were generated. The best model was selected on the basis of a high correlation coefficient (r), lowest total cost, and RMSD values. The final model was further validated by a test set of 119 molecules.

2.4. Generation of pharmacophore model

From the structures of the training set compounds and their experimentally determined inhibitory activities against p38 MAP kinase, 10 best pharmacophore (or hypotheses) models

were generated using HypoGen module implemented in Catalyst 4.10 software. An initial analysis revealed that three chemical feature types such as hydrogen-bond acceptor (HA), hydrophobic (HY), and two ring aromatic (RA) features could effectively map all critical chemical features of all molecules in the training and test sets. These features were selected and used to build a series of hypotheses with the HypoGen module in Catalyst using default uncertainty value 3 (defined by Catalyst as the measured value being within three times higher or three times lower of the true value). Catalyst generates a chemical feature based model on the basis of the most active compounds. In hypothesis generation, the structure and activity correlations in the training set were rigorously examined. HypoGen identifies features that were common to the active compounds but excluded from the inactive compounds within conformationally allowable regions of space. It further estimates the activity of each training set compound using regression parameters. The parameters are computed by the regression analysis using the relationship of geometric fit value versus the negative logarithm of activity. The greater the geometric fit, the greater the activity prediction of the compound. The fit function does not only check if the feature is mapped or not, it also contains a distance term, which measures the distance that separates the feature on the molecule from the centroid of the hypothesis feature. Both terms are used to calculate the geometric fit value.

2.5. Pharmacophore validation

The generated pharmacophore model should predict activity of the molecules accurately, and should identify active compound from a database. Therefore, the derived pharmacophore map was validated using (i) cost analysis, (ii) test set prediction and (iii) Fisher's test.

2.6. Cost analysis

The HypoGen module in Catalyst performs two important theoretical cost calculations that determine the success of any pharmacophore hypothesis. One is the 'fixed cost' (also termed as ideal cost), which represents the simplest model that fits all data perfectly, and the second one is the 'null cost' (also termed as no correlation cost), which represents the highest cost of a pharmacophore with no features and estimates activity to be the average of the activity data of the training set molecules. A meaningful pharmacophore hypothesis may result when the difference between null and fixed cost value is large; a value of 40–60 bits for a pharmacophore hypothesis may indicate that it has 75–90% probability of correlating the data (Catalyst 4.10 documentation).

Two other parameters also determine the quality of any pharmacophore – configuration cost or entropy cost, which depends on the complexity of the pharmacophore hypothesis space and should have a value <17, and the error cost, which is dependent on the root mean square differences between the estimated and the actual activities of the training set molecules. The RMSD represents the quality of the correlation between the estimated and the actual activity data. The best pharmacophore model has highest cost difference, lowest RMSD and best correlation coefficient.

2.7. Test set activity prediction

In addition to estimation of activity of training set molecules, the pharmacophore model should also estimate the activity of new compounds. For external validation of the pharmacophore model we have considered 119 compounds as test set (Table 1S), having wide range of activities (IC_{50}, spanning from 0.2 to 13 00 000 nM) and structural diversity. The best pharmacophore (Hypo1) having high correlation coefficient (r), lowest total cost, and lower RMSD value was chosen to estimate the activity of test set. Test set compounds were classified on the basis of their activity as highly active (<10 nM, +++), moderately active (10–100 nM, ++), and inactive (>100 nM, +).

2.8. Fisher's test

Using the module CatScrambe, the molecular spreadsheets of our training set were modified by arbitrary scrambling of the affinity data for all compounds. These randomized spreadsheets should yield hypotheses without statistical significance; otherwise, the original model is also random. To achieve a statistical significance level of 98%, 49 random spreadsheets were generated for each of our three hypotheses. For all three targets, randomization tests gave hypotheses with total cost values lying well above those reported for the sets of original hypotheses, yielding lower values for the differences null hypothesis cost – total cost, further supporting the statistical significance of our models.

3. Results and discussion

Pharmacophore models were generated by HypoGen present in Catalyst 4.10 [28] and top 10 hypotheses (Table 1) were exported finally. Most hypotheses have high correlation (>0.86). Interestingly, eight out of 10 best hypotheses have same four features: one hydrogen-bond acceptor, two hydrophobic aromatic and one hydrophobic feature (Fig. 1), which shows the stability of the hypotheses, in other words, reliability. On the basis of the very similar composition of the 10 hypotheses, hypothesis 1 (Hypo1), characterized by the best statistical parameters (Table 1) in terms of its predictive ability, as indicated by the highest correlation coefficient and lowest RMS deviations, has been chosen to represent 'the pharmacophore model'. Remarkably, the highest active compound (compound **31**, Table 2) can be nicely mapped onto the Hypo1 model by the best fit values, which are shown in Fig. 2(A), indicating that the Hypo1 model provides reasonable pharmacophoric characteristics of the p38 MAP kinase inhibitors for components of their activities.

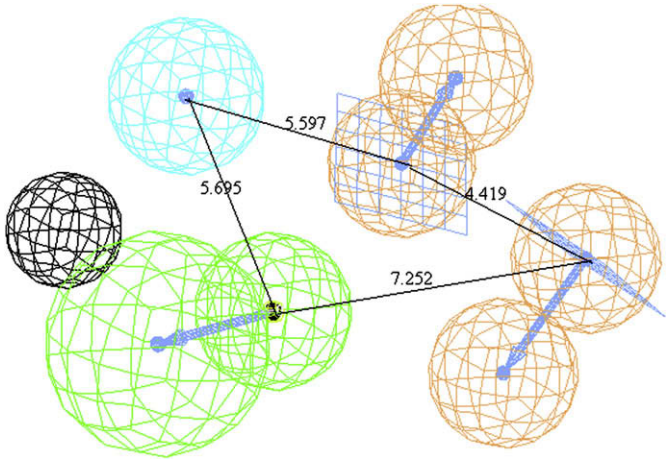

Fig. 1. The best hypothesis model Hypo1 produced by the HypoGen module in Catalyst 4.10 software.

3.1. Cost analysis

In addition to generating a hypothesis, Catalyst also provides two theoretical costs (represented in bit units) to help assess the validity of the hypothesis. The first is the cost of an ideal hypothesis (fixed cost), which represents the simplest model that fits all data perfectly. The second is the cost of the null hypothesis (null cost), which represents the highest cost of a pharmacophore with no features and which estimates activity to be the average of the activity data of the training set molecules. They represent the upper and lower bounds for the hypotheses that are generated. A generated hypothesis with a score that is substantially below that of the null hypothesis is likely to be statistically significant and bears visual inspection. The greater the difference between the cost of the generated hypothesis and the cost of the null hypothesis, the less likely it is that the hypothesis reflects a chance correlation. A value of 40–60 bits between them for a pharmacophore hypothesis may indicate that it has 75–90% probability of correlating the data. The total fixed cost of the run is 116.569, the cost of the null hypothesis is 305.792, and the total cost of the Hypo1 is 141.995 (Table 1). Then, the cost range between Hypo1 and the fixed cost is 25.426, while that between the null hypothesis and Hypo1 is 163.797 (Table 1), which shows that Hypo1 has more than 90% probability of correlating the data. Noticeably, the total cost of Hypo1 was much closer to the fixed cost than to the null cost. Furthermore, a high correlation coefficient of 0.959 was observed with RMS value of 1.069 and the configuration cost of 14.536, demonstrating that we have successfully developed a reliable pharmacophore model with high predictivity.

3.2. Score hypothesis

To verify Hypo1's discriminability among p38 MAP kinase inhibitors with different order of magnitude activity, all training set compounds were classified by their activity as highly active (<10 nM, +++), moderately active (10–100 nM, ++), and inactive (>100 nM, +). The actual and estimated p38 MAP kinase inhibitory activities of the 30 compounds based on Hypo1 are listed in Table 2. All the eight compounds except compounds **36** and **17** were classified correctly in high active range (Table 2). The discrepancy between the actual and the estimated activity observed for the two compounds was only about one-order of magnitude, which might be an artifact of the program that uses different numbers of degrees of freedom for these compounds to mismatch the pharmacophore model. The error factor is also reported in Table 2. It shows that 29 molecules out of the 30 molecules in the training set have errors less than 10 which means that the activity prediction of these compounds falls between 10-fold greater and 1/10 of the actual activity, while the remaining one (compound **34**) has errors 14.0. In this compound, the second RA is not

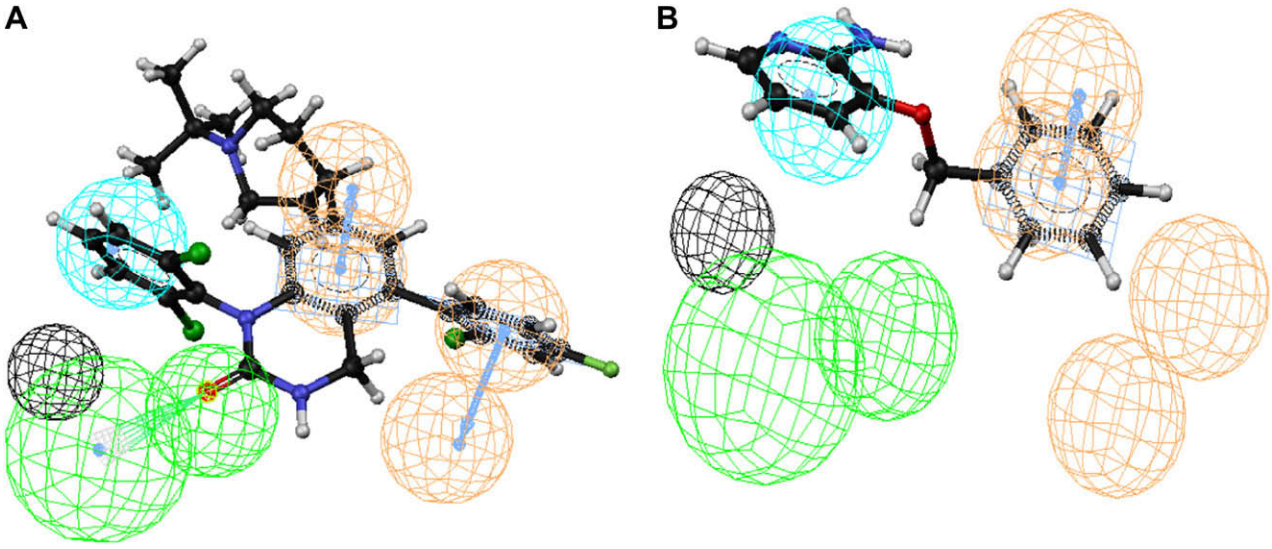

Fig. 2. (A) Pharmacophore mapping of the most active compound on the best hypothesis model Hypo1. Compound **31** from the training set. (B) Pharmacophore mapping of the least active compound on the best hypothesis model Hypo1. Compound **66** from the training set.

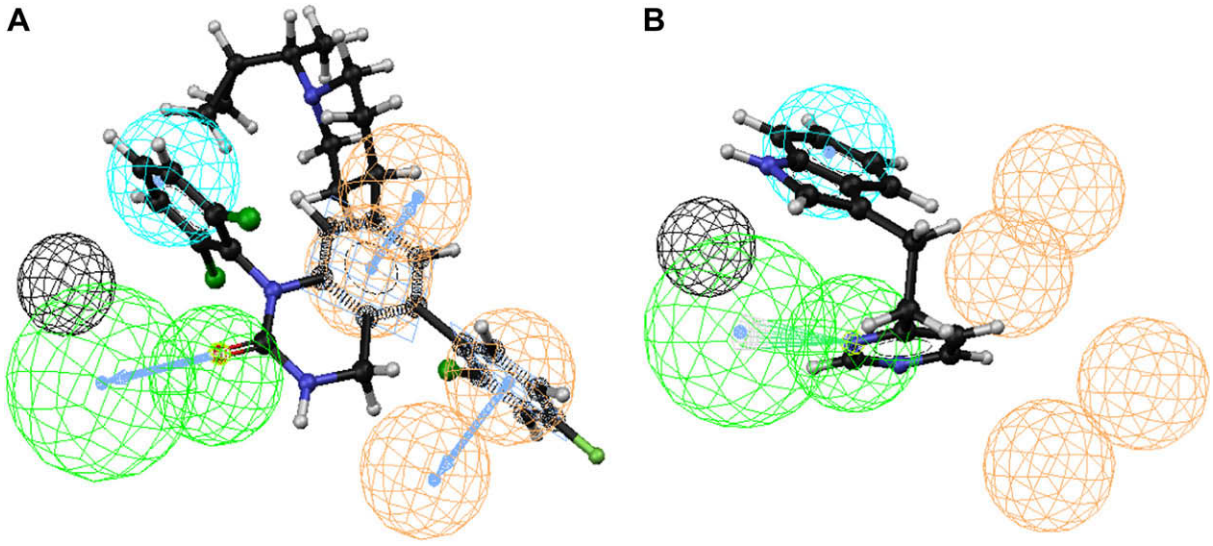

Fig. 3. (A) Pharmacophore mapping of the most active compound on the best hypothesis model Hypo1. Compound **28** from the test set. (B) Pharmacophore mapping of the least active compound on the best hypothesis model Hypo1. Compound **76** from the test set.

mapping may be due to more flexibility of the compound that it is hard to find true active conformation in prediction, which may be the reason for its underestimated value. These results confirm that our hypothesis is a reliable model for describing the SAR in the training set.

In this study, all but one highly active compound map the hydrogen-bond acceptor (HA) feature, and one least active inhibitor do not have this feature. Furthermore, HA maps on CO of quinazoline ring (Fig. 3).

3.3. Validation of the constructed pharmacophore model

The actual activity versus estimated activity of the 119 compounds in the test is shown in Table S1 in the Supporting information. A correlation coefficient of 119 generated using the test set compounds shows a good correlation of 0.851 between the actual and the estimated activities. Detailed, 15 out of 17 highly active (88.3), 33 of 40 moderately active (82%), and 20 of 25 inactive compounds (81%) were predicted correctly. Two highly active compounds were underestimated as moderately active; five moderately active compounds were underestimated as inactive and other seven moderately active compounds were overestimated as highly active; most of inactive compounds were overestimated as moderately active. In conclusion, most of the compounds in the test set were predicted correctly, which mean the hypothesis is suited for screening high active compounds from the database. The mapping of test compound **38** on Hypo1 is shown in Fig. 3(A).

3.4. Fisher's test

To further evaluate the statistical relevance of the model, Fisher's method was applied. With the aid of the CatScramble program, the experimental activities in the training set were scrambled randomly, and the resulting training set was used for a HypoGen run (Fig. 4). All parameters were adopted which were used in initial HypoGen calculation. This procedure was reiterated 49 times. None of the outcome hypotheses has lower cost score than the initial hypothesis. Ten lowest

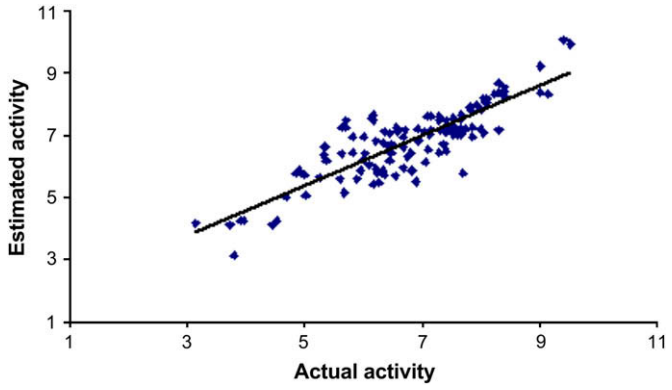

Fig. 4. Correlation graph between experimental and Hypo1-estimated activities of test set.

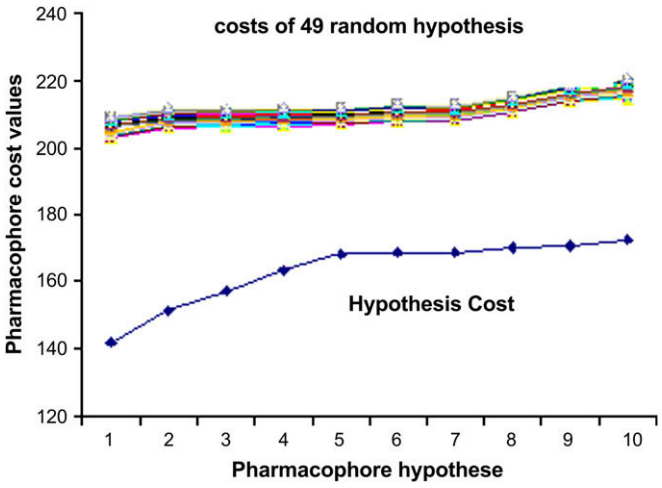

Fig. 5. The difference in costs between the HypoGen runs and the scrambled runs.

total cost values of the resulting 49 hypotheses was compared with our hypothesis costs. None of the costs of the scrambled hypothesis was less than our hypothesis costs (Fig. 5). These results indicates that there is a 98% chance for the best hypothesis to represent a true correlation in the training set activity data. Furthermore, all the top 10 hypotheses exported by HypoGen pass 98% Fisher's test indicate that the models are not random, but meaningful and successful.

4. Conclusion

A data set of 149 compounds of selective p38 MAPK inhibitors whose chemical features along with their respective activities ranging over a wide range of magnitude is used to generate pharmacophore hypotheses to successfully and accurately predict the activity. A highly predictive pharmacophore model was generated based on 30 training set molecules, which had hydrogen-bond acceptor, hydrophobic, hydrophobic bond donor and ring aromatic as chemical features which described their activities towards p38 MAP kinase. The validity of the model was based on 119 test set molecules, which finally showed that the model was able to accurately differentiate various classes of p38 MAPK inhibitors with a high correlation coefficient of 0.851 between experimental and predicted activity. This validated pharmacophore model, as such can be used as a query for identification of potential inhibitors of p38 MAP kinase while it can also be used to validate the potential of the compound to inhibit the enzyme prior to taking any step regarding the synthesis. Thus, we hope that the model generated will be helpful to identify novel and potential lead molecules with improved activity against p38 MAP kinases.

Acknowledgements

The authors thank Dr. J.A.R.P. Sarma, Senior Vice President and Dr. K.V. Radhakishan, Director, GVK Biosciences Pvt. Ltd. for their cooperation and providing software facilities.

Appendix. Supplementary data

Supplementary data associated with this article can be found, in the online version, at doi:10.1016/j.ejmech.2008.02.014.

References

[1] F.M. Brennan, M. Feldman, Curr. Opin. Immunol. (1996) 872–877.
[2] G. Camussi, E. Lupia, Drugs 55 (1998) 613–620.
[3] Catalyst 4.10, Accelrys, Inc., San Diego, CA, 2005.<http://www.accelrys.com/>.
[4] F.F. Oliver, K. Viktor, D. Jan, L.J. Thierry, J. Med. Chem. 47 (2004) 2750.
[5] J.E. Stelmach, L. Liu, S.B. Patel, J.V. Pivnichny, G. Scapin, S. Singh, C.E. Hop, Z. Wang, J.R. Strauss, P.M. Cameron, E.A. Nichols, S.J. O'Keefe, E.A. O'Neill, D.M. Schmatz, C.D. Schwartz, C.M. Thompson, D.M. Zaller, J.B. Doherty, Bioorg. Med. Chem. Lett. 13 (2003) 277–280.
[6] D.C. Underwood, R.R. Osborn, C.J. Kotzer, J.L. Adams, J.C. Lee, E.F. Webb, D.C. Carpenter, S. Bochnowicz, H.C. Thomas, D.W. Hay, D.E. Griswold, J. Pharmacol. Exp. Ther. 293 (2000) 281–288.
[7] K.C. Rupert, J.R. Henry, J.H. Dodd, S.A. Wadsworth, D.E. Cavender, G.C. Olini, B. Fahmy, J.J. Siekierka, Bioorg. Med. Chem. Lett. 13 (2003) 347–350.
[8] S.L. Colletti, J.L. Frie, E.C. Dixon, S.B. Singh, B.K. Choi, G. Scapin, C.E. Fitzgerald, S. Kumar, E.A. Nichols, S.J. O'Keefe, E.A. O'Neill, G. Porter, K. Samuel, D.M. Schmatz, C.D. Schwartz, W.L. Shoop, C.M. Thompson, J.E. Thompson, R. Wang, A. Woods, D.M. Zaller, J.B. Doherty, J. Med. Chem. 46 (2003) 349–352.
[9] A.L. Gill, M. Frederickson, A. Cleasby, S.J. Woodhead, M.G. Carr, A.J. Woodhead, M.T. Walker, M.S. Congreve, L.A. Devine, D. Tisi, M. O'Reilly, L.C. Seavers, D.J. Davis, J. Curry, R. Anthony, A. Padova, C.W. Murray, R.A. Carr, H. Jhoti, J. Med. Chem. 48 (2005) 414–426.
[10] S.A. Wadsworth, D.E. Cavender, S.A. Beers, P. Lalan, P.H. Schafer, E.A. Malloy, W. Wu, B. Fahmy, G.C. Olini, J.E. Davis, J.L. Pellegrino-Gensey, M.P. Wachter, J.J. Siekierka, J. Pharmacol. Exp. Ther. 291 (1999) 680–687.
[11] M.A. Dombroski, M.A. Letavic, K.F. McClure, J.T. Barberia, T.J. Carty, S.R. Cortina, C. Csiki, A.J. Dipesa, N.C. Elliott, C.A. Gabel, C.K. Jordan, J.M. Labasi, W.H. Martin, K.M. Peese, I.A. Stock, L. Svensson, F.J. Sweeney, C.H. Yu, Bioorg. Med. Chem. Lett. 14 (2004) 919–923.
[12] P.F. Cirillo, C. Pargellis, J. Regan, Curr. Top. Med. Chem. 2 (2002) 1021–1035.
[13] Z. Wan, J.C. Boehm, M.J. Bower, S. Kassis, J.C. Lee, B. Zhao, J.L. Adams, Bioorg. Med. Chem. Lett. 13 (2003) 1191–1194.
[14] L. Revesz, F.E. Di Padova, T. Buhl, R. Feifel, H. Gram, P. Hiestand, U. Manning, A.G. Zimmerlin, Bioorg. Med. Chem. Lett. 10 (2000) 1261–1264.
[15] L. Revesz, F.E. Di Padova, T. Buhl, R. Feifel, H. Gram, P. Hiestand, U. Manning, R. Wolf, A.G. Zimmerlin, Bioorg. Med. Chem. Lett. 12 (2002) 2109–2112.
[16] T.A. Engler, K. Furness, S. Malhotra, C. Sanchez-Martinez, C. Shih, W. Xie, G. Zhu, X. Zhou, S. Conner, M.M. Faul, K.A. Sullivan, S.P. Kolis, H.B. Brooks, B. Patel, R.M. Schultz, T.B. DeHahn, K. Kirmani, C.D. Spencer, S.A. Watkins, E.L. Considine, J.A. Dempsey, C.A. Ogg, N.B. Stamm, B.D. Anderson, R.M. Campbell, V. Vasudevan, M.L. Lytle, Bioorg. Med. Chem. Lett. 13 (2003) 2261–2267.
[17] S.E. de Laszlo, D. Visco, L. Agarwal, L. Chang, J. Chin, G. Croft, A. Forsyth, D. Fletcher, B. Frantz, C. Hacker, W. Hanlon, C. Harper, M. Kostura, B. Li, S. Luell, M. MacCoss, N. Mantlo, E.A. O'Neill, C. Orevillo, M. Pang, J. Parsons, A. Rolando, Y. Sahly, K. Sidler, S.J. O'Keefe, et al., Bioorg. Med. Chem. Lett. 8 (1998) 2689–2694.
[18] J.L. Adams, J.C. Boehm, T.F. Gallagher, S. Kassis, E.F. Webb, R. Hall, M. Sorenson, R. Garigipati, D.E. Griswold, J.C. Lee, Bioorg. Med. Chem. Lett. 11 (2001) 2867–2870.
[19] B.J. Mavunkel, S. Chakravarty, J.J. Perumattam, G.R. Luedtke, X. Liang, D. Lim, Y.J. Xu, M. Laney, D.Y. Liu, G.F. Schreiner, J.A. Lewicki, S. Dugar, Bioorg. Med. Chem. Lett. 13 (2003) 3087–3090.
[20] L. Revesz, E. Blum, F.E. Di Padova, T. Buhl, R. Feifel, H. Gram, P. Hiestand, U. Manning, G. Rucklin, Bioorg. Med. Chem. Lett. 14 (2004) 3595–3599.
[21] L. Revesz, E. Blum, F.E. Di Padova, T. Buhl, R. Feifel, H. Gram, P. Hiestand, U. Manning, G. Rucklin, Bioorg. Med. Chem. Lett. 14 (2004) 3601–3605.
[22] L. Liu, J.E. Stelmach, S.R. Natarajan, M.H. Chen, S.B. Singh, C.D. Schwartz, C.E. Fitzgerald, S.J. O'Keefe, D.M. Zaller, D.M. Schmatz, J.B. Doherty, Bioorg. Med. Chem. Lett. 13 (2003) 3979–3982.
[23] J.G. Cumming, C.L. McKenzie, S.G. Bowden, D. Campbell, D.J. Masters, J. Breed, P.J. Jewsbury, Bioorg. Med. Chem. Lett. 14 (2004) 5389–5394.
[24] S.A. Laufer, W. Zimmermann, K.J. Ruff, J. Med. Chem. 47 (2004) 6311–6325.
[25] B.R. Brooks, R.E. Bruccoleri, B.D. Olafson, D.J. States, S. Swaminathan, M. Karplus, J. Comp. Chem. 4 (1983) 187.
[26] J. Gasteiger, M. Marsilli, Tetrahedron 36 (1980) 3219.
[27] J.J.J. Stewart, Comput. Aided Mol. Des. 4 (1990) 1.
[28] MSI Cerius2 Version 4.9, Molecular Simulations, Accelrys Inc., 9685 Scranton Rd., San Diego, CA 92121, USA.